Equilibrium of EuS with Gas Mixtures of H_2S, H_2 and CO_2

J. Hauck

Institut für Festkörperforschung, Kernforschungsanlage Jülich, West Germany

Z. Naturforsch. **37a**, 1309–1314 (1982); received November 12, 1981

EuS and Eu_2O_3 powder samples were equilibrated with H_2S-H_2-CO_2 gas mixtures in the temperature range 700–1500 °C. Since the sulfur and oxygen fugacities of the gas mixtures — as calculated from thermodynamic data — can vary by about 10^7, EuS of different stoichiometries may be produced. At higher oxygen and lower sulfur fugacities EuS is oxidized to Eu_2O_2S. The border line between the two phases can be fitted by the equation $\log(f(S_2)/\text{atm.}) = 2\log(f(O_2)/\text{atm.}) + 48300/T - 9.3$ and compared to border lines of other phases of the Eu-O-S system, which can be calculated from thermodynamic data.

Introduction

The consideration of oxygen contamination is particularly important for sulfides of elements which are very sensitive to oxidation, such as the rare earth elements. Depending on the kind of preparation samples of different compositions may be obtained. EuS e.g. has been prepared (a) from the elements [1–3], (b) from Eu_2O_3 and CS_2 [4], (c) from Eu-oxalate [5], -citrate [6], -sulfate [7], -sulfite [8], -chloride [9] or oxide [10, 11] and H_2S, (d) from $EuSO_4$ and C [5]. Such samples exhibit different physical properties like the conductivity [1, 10], which are sensitive to small changes in stoichiometry. The different sulfides can be equilibrated to samples of well defined composition in a gas-solid reaction with a gas mixture of H_2S, H_2 and CO_2. The sulfur and oxygen fugacities * of this mixture can vary by about 10^7 (Table 1) [12] giving rise to different stoichiometries of the sulfide.

Experimental Methods

99.99% Eu_2O_3 powder was used as starting material for most runs. Charges of about 70 mg Eu_2O_3 in corundum crucibles were equilibrated at 700, 900, 1100, 1300 and 1500 °C in a flowing gas mixture at 1 atm. total pressure. A vertical tube furnace with "Kanthal"-winding was used for 700–1100 °C, with Rh-winding for the runs at 1300 and 1500 °C. A glass fitting attached to the bottom of the corundum tube served as the gas inlet. Atmospheres of desired oxygen and sulfur pressures in the furnace were obtained by mixing high purity gases of H_2S, H_2 and CO_2 in a gas flowmeter [13]. The H_2 was supplied from a steel container with $FeTiH_x$ filling [14], where a higher purity than in conventional hydrogen reservoirs can be achieved. Controlled flow rates of the gases could be obtained above ~ 0.03 ml/sec by calibrated capillaries [13]. The calibration curves were nearly linear at flow rates up to 6 ml/sec, which was chosen as the maximum total flow rate in the corundum tube with the diameter 2.8 cm. This flow rate minimizes thermal diffusion and temperature uncertainties and provides for a slightly positive furnace exit pressure [13]. The minor gas constituent of the experiments exceeded 0.5 volume percent. At this level, contamination of the gases is of minor importance though the oxygen and sulfur fugacities of the reacting gas mixtures can be as low as e.g. 10^{-22} and 10^{-8} atm. at 900 °C (Table 1). Usually the mixing ratio of H_2S and H_2 $y = \log([H_2S]/[H_2])$ was kept constant and the mixing ratio of CO_2 and H_2 $x = \log([CO_2]/[H_2])$ was changed in steps of $\Delta x = 0.1$. The actual $f(O_2)$ and $f(S_2)$ fugacities of these mixtures were obtained by graphical interpolation of the values in Table 1.

The temperature in the furnace was kept constant to within ±3 °C by means of commercial electronic controllers. The actual temperatures were measured with a Pt-90 pct Pt-10 pct Rh thermocouple which was checked periodically against a calibrated reference thermocouple. The samples were kept for 1–3 hours in the hot zone of the furnace and then pulled out to the cold end of the corundum tube. In order to check that true equi-

* The thermodynamically more rigorous term fugacity is used in preference to partial pressure, since only at high temperatures and low total pressures these two terms are essentially equivalent.

Reprint requests to Dr. J. Hauck, Institut für Festkörperforschung, Kernforschungsanlage Jülich, 5170 Jülich.

0340-4811 / 81 / 1200-1309 $ 01.00/0. — Please order a reprint rather than making your own copy.

Table 1. $-\log f(S_2)$ (upper value) and $-\log f(O_2)$ (lower value) of H_2S-H_2-CO_2 gas mixtures at the mixing ratios $x = \log([CO_2]/[H_2])$ and $y = \log([H_2S]/[H_2])$ and 1 atm. total pressure.

$-\log f(S_2)$ / $-\log f(O_2)$	$y=-3$	$y=-2$	$y=-1$	$y=0$	$y=1$	$y=2$	$y=3$
700 °C							
$x=-3$	10.56	8.56	6.56	4.56	2.64	1.89	1.82
	26.22	26.22	26.22	26.25	26.36	27.50	—
$x=-2$	10.53	8.53	6.53	4.54	2.64	1.89	1.82
	24.28	24.28	24.29	24.42	24.58	25.54	27.43
$x=-1$	10.41	8.41	6.42	4.46	2.60	1.89	1.82
	22.57	22.58	22.60	22.74	22.85	23.74	25.47
$x=0$	10.07	8.07	6.07	4.09	2.36	1.86	1.81
	21.01	21.01	21.01	21.02	21.09	22.09	23.66
$x=1$	8.98	6.97	4.99	3.11	1.95	1.74	1.79
	19.19	19.19	19.19	19.20	19.52	20.56	22.02
$x=2$	8.11	6.12	4.25	2.81	1.98	1.65	1.69
	17.23	17.24	17.28	17.55	18.30	19.26	20.51
$x=3$	—	10.68	8.27	4.66	2.64	1.90	1.62
	15.24	15.25	15.46	16.34	17.19	18.20	19.24
900 °C							
$x=-3$	8.91	6.91	4.91	2.92	1.48	1.26	1.24
	22.02	22.02	22.04	22.08	22.24	23.91	—
$x=-2$	8.90	6.90	4.90	2.91	1.48	1.26	1.24
	20.23	20.23	20.23	20.24	20.45	21.96	23.89
$x=-1$	8.82	6.83	4.83	2.84	1.46	1.26	1.24
	18.26	18.26	18.26	18.26	18.70	20.17	21.94
$x=0$	8.28	6.28	4.29	2.37	1.37	1.25	1.24
	16.18	16.18	16.18	16.20	16.86	18.44	20.14
$x=1$	7.01	5.02	3.18	1.85	1.24	1.18	1.23
	14.09	14.09	14.12	14.38	15.26	16.66	18.41
$x=2$	10.43	8.38	6.00	2.92	1.59	1.15	1.17
	12.08	12.10	12.30	13.06	13.93	15.16	16.64
$x=3$	—	14.39	11.97	8.02	3.08	1.57	1.14
	10.09	10.11	10.32	11.28	12.89	13.88	15.15
1100 °C							
$x=-3$	7.73	5.73	3.74	1.84	1.02	0.93	0.92
	19.02	19.02	19.02	18.90	19.58	21.38	—
$x=-2$	7.73	5.73	3.73	1.83	1.02	0.93	0.92
	17.04	17.04	17.04	17.06	17.82	19.43	21.32
$x=-1$	7.65	5.65	3.66	1.78	1.02	0.93	0.92
	15.00	15.00	15.00	15.06	16.04	17.67	19.42
$x=0$	7.00	5.01	3.05	1.49	0.99	0.92	0.92
	12.73	12.73	12.74	12.94	14.10	15.90	17.66
$x=1$	7.19	5.17	3.12	1.62	0.97	0.90	0.92
	10.48	10.51	10.65	11.14	12.26	13.98	15.88
$x=2$	13.02	10.98	8.58	4.63	1.59	0.93	0.89
	8.44	8.47	8.67	9.66	10.84	12.17	13.96
$x=3$	—	17.00	14.58	10.62	5.06	1.59	0.92
	6.44	6.46	6.67	7.65	9.44	10.81	12.17
1300 °C							
$x=-3$	6.86	4.86	2.89	1.27	0.79	0.74	0.73
	16.62	16.62	16.62	16.62	17.61	19.38	—
$x=-2$	6.85	4.85	2.88	1.27	0.79	0.74	0.73
	14.62	14.62	14.62	14.77	15.86	17.49	19.37
$x=-1$	6.78	4.78	2.82	1.25	0.79	0.74	0.73
	12.57	12.57	12.57	12.78	14.04	15.76	17.48
$x=0$	6.08	4.10	2.32	1.17	0.79	0.74	0.73
	10.18	10.18	10.22	10.63	12.05	13.93	15.75
$x=1$	8.96	6.90	4.50	1.76	0.86	0.74	0.73
	7.78	7.81	8.03	8.80	10.01	11.94	13.92
$x=2$	14.95	12.91	10.52	6.54	1.85	0.83	0.73
	5.73	5.76	5.96	6.96	8.60	9.94	11.94
$x=3$	—	18.57	16.29	12.54	6.98	1.86	0.83
	3.92	3.92	4.06	4.94	6.73	8.57	9.93
1500 °C							
$x=-3$	6.20	4.21	2.31	1.01	0.67	0.64	0.63
	14.75	14.75	14.74	14.91	16.02	17.74	—
$x=-2$	6.19	4.20	2.31	1.01	0.68	0.64	0.63
	12.74	12.74	12.75	13.04	14.29	15.92	17.81
$x=-1$	6.12	4.13	2.26	1.01	0.68	0.64	0.63
	10.70	10.70	10.71	11.05	12.42	14.20	15.92
$x=0$	5.54	3.62	2.04	1.03	0.69	0.64	0.63
	8.20	8.21	8.29	8.86	10.42	12.33	14.19
$x=1$	10.42	8.36	5.94	2.18	0.83	0.65	0.64
	5.70	5.72	5.94	7.00	8.27	10.33	12.32
$x=2$	16.36	14.32	12.00	8.02	2.44	0.81	0.65
	3.68	3.70	3.88	4.86	6.78	8.20	10.32
$x=3$	—	18.05	16.00	13.47	8.46	2.48	0.80
	2.83	2.83	2.86	3.12	4.64	6.76	8.20

librium was attained, the final state was approached from different starting materials.

The quenched samples were microscopically examined in reflected light, where EuS (black), impurities of unreacted Eu_2O_3 (white) and the oxidation product Eu_2O_2S (light yellow) could be identified. The lattice parameters of the samples were calculated from x-ray powder patterns, which were measured on a powder diffractometer by step scanning with $a(Au) = 4.0786$ Å as internal standard.

Results

EuS could be obtained from Eu_2O_3 in about half of the experimentally possible range of different mixing ratios of x and y ($x = \log([CO_2]/[H_2])$, $y = \log([H_2S]/[H_2])$). At the higher oxygen or lower sulfur fugacities Eu_2O_2S was obtained as oxidation product (e.g. Fig. 1 for 900 °C). The experimentally determined oxygen and sulfur fugacities of the border line are listed in Table 2. Within the experimental uncertainties they can be fitted to a straight line by the equation

$$\log(f(S_2)/\text{atm}) = 2\log(f(O_2)/\text{atm}) = 48300(\pm 930)/T - 9.3(\pm 0.7).$$

These values can be interpreted by a temperature independent reaction enthalpy of $\Delta H = -925 \pm 18$ kJ g-mol^{-1} and entropy $\Delta S = -178 \pm 14$ J · g-mol^{-1} deg^{-1} for the reaction

$$4\,EuS + 2\,O_2 \rightarrow 2\,Eu_2O_2S + S_2$$

with the reaction constant $K = f(S_2)/f^2(O_2)$ and the Gibbs free energy

$$\Delta G = \Delta H - T\Delta S = -2.303\,RT \log K.$$

The experimental values can be compared with values of other Eu-O-S-phases whose existence range can be calculated from thermodynamic data. Figure 1 exhibits the Eu-O-S phases at 900 °C for different $f(O_2)$ and $f(S_2)$ fugacities. The slopes of the straight border lines I—IX are given by the coefficients of O_2 and S_2 in the chemical reaction equations I—X, if stoichiometric compounds are assumed to a first approximation:

I)	$2\,Eu + O_2 \rightarrow 2\,EuO$	$\log f(O_2) = -43.47$,
II)	$6\,EuO + O_2 \rightarrow 2\,Eu_3O_4$	$\log f(O_2) = -30.57$,
III)	$4\,Eu_3O_4 + O_2 \rightarrow 6\,Eu_2O_3$	$\log f(O_2) = -25.56$,
IV)	$2\,Eu + S_2 \rightarrow 2\,EuS$	$\log f(S_2) = -36.75$,
V)	$2\,EuS + O_2 \rightarrow 2\,EuO + S_2$	$\log f(S_2) - \log f(O_2) = 6.72$,
VI)	$3\,EuS + 2\,O_2 \rightarrow Eu_3O_4 + \frac{3}{2}S_2$	$\frac{3}{2}\log f(S_2) - 2\log f(O_2) = 25.37$,
VII)	$2\,EuS + \frac{3}{2}O_2 \rightarrow Eu_2O_3 + S_2$	$\log f(S_2) - \frac{3}{2}\log f(O_2) = 21.17$,
VIII)	$4\,EuS + 2\,O_2 \rightarrow 2\,Eu_2O_2S + S_2$	$\log f(S_2) - 2\log f(O_2) = 31.88$,
IX)	$2\,Eu_2O_2S + O_2 \rightarrow 2\,Eu_2O_3 + S_2$	$\log f(S_2) - \log f(O_2) = 10.47$,
X)	$6\,EuS + S_2 \rightarrow 2\,Eu_3S_4$	$\log f(S_2) = -0.5$.

The absolute values of the straight lines of the $\log f(O_2)/\log f(S_2)$ plot were calculated from the following values of the Gibbs free energy at 1173 K:

Substance	G^{1173} (kJ/gfw) *	Reference
Eu	− 105.1	[15], or interpolated between the values for Gd and Sm [16]
O_2	− 263.64	[16]
S_2	− 164.54	[16]
EuO	− 725.32	[17]
Eu_3O_4	− 2651.21	value of [17] at the upper limit of uncertainty
Eu_2O_3	− 1907.15	[17]
EuS	− 600.25	[16]
Eu_2O_2S	− 1739.98	from experimental values of this investigation
Eu_3S_4	− 1889	estimated value

* 1 cal = 4.187 J.

The minimum values of $\log f(O_2)$ and $\log f(S_2)$ are chosen at the stability field of Eu as is shown in Figure 1. Proceeding along the sulfur axis, one passes from the field of metallic Eu to that of EuS and then to that of Eu_3S_4. At still higher sulfur fugacities sulfur condenses. Since the experimental temperature is above the melting point of sulfur, the condensed sulfur will be present in the liquid state. No further increase in sulfur fugacity is possible since any attempted increase merely results in a further precipitation of liquid sulfur. The appearance of condensed sulfur thus represents the upper limit of the sulfur fugacity at this temperature (900 °C). Proceeding along the oxygen axis, one passes from the stability field of Eu directly into that of EuO. At still higher oxygen fugacities the

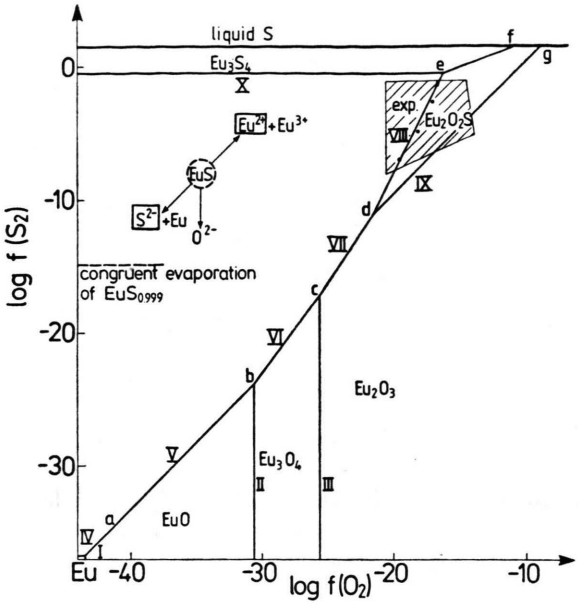

Fig. 1. Phases of the Eu-O-S system at 900 °C and with different $f(S_2)$ and $f(O_2)$-fugacities as determined from thermodynamic data and experimental values (dashed area). The incorporation of different lattice defects is sketched for EuS. Letters indicate the $f(S_2)/f(O_2)$ values of the three phase fields of Fig. 3 I, roman numbers the lines for chemical reactions I—X (see text).

Table 2. $\log f(S_2)$ and $\log f(O_2)$ values for the phase boundary EuS/Eu_2O_2S as determined at 700, 900, 1100, 1300 and 1500 °C.

T(K)	$-\log f(S_2)$	$-\log f(O_2)$
973	4.5	22.6
1173	1.2	16.6
	1.4	16.7
	2.6	17.0
	4.8	18.1
	6.9	19.5
1373	1.4	13.5
1573	0.8	11.3
	1.3	11.2
	4.8	13.1
1773	1.1	9.5

Eu_3O_4 and Eu_2O_3 fields are reached. There is no upper boundary imposed on the oxygen fugacity as by the condensation of sulfur, since the experimental temperature is higher than the critical temperature of oxygen. In this investigation with a main interest on the upper limit of the existence of Eu^{2+}, the oxygen fugacities of H_2S-H_2-CO_2 mixtures were taken as upper limit. The phase boundary between Eu_2O_2S and Eu_2O_3, as calculated from thermodynamic data, could be affirmed qualitatively by some runs at high CO_2 and low H_2S content of the gas mixture. At these conditions the reaction of Eu_2O_3 to Eu_2O_2S and the reversed reaction were quite sluggish, giving rise to some uncertainties for a quantitative determination of the border line. At 1 atm. O_2, EuS is oxidized to $Eu_2O_2SO_4$ [4, 18]. The intermediate Eu-sulfates and oxysulfates are not included in this investigation, because of experimental difficulties to vary oxygen and sulfur fugacities at higher values. Somewhat greater oxygen fugacities can be obtained by substituting SO_2-H_2-CO_2 mixtures [19] and in the present study were only used in the H_2S-H_2-CO_2 mixtures range to check the correctness of the later's experiments.

Figure 2 A—C show how the hypothetical phase relations change by use of other thermodynamic data. In Fig. 2A the energies of formation of Eu_3O_4 and Eu_2O_2S of [17] were used for calculations of $G^{1173}(Eu_3O_4) = -2626.09$ and $G^{1173}(Eu_2O_2S) = -1823.49$ kJ/gfw, respectively. At this condition the Gibbs free energy of the reaction

$$EuO + Eu_2O_3 \rightarrow Eu_3O_4 \quad \Delta G = 6.38\,\text{kJ/gfw}$$

become positive, that means Eu_3O_4 would be decomposed to EuO and Eu_2O_3, which is in contrast to the phase diagrams of ref. [20—22]. The more negative value of Eu_2O_2S would imply a Eu_2O_2S field enlarged over the whole experimentally determined area. In Fig. 2B the more negative Gibbs free energy of Eu_2O_3 — 1996.70 kJ/gfw of ref. [16] enlarges the Eu_2O_3 field even more in relation to the EuO, EuS and Eu_2O_2S fields and Eu_2O_3 would have been expected in the experimental area. McCarthy and White [22] estimate about the same value for EuO but with larger values — 2720 and — 1948 kJ/gfw for Eu_3O_4 and Eu_2O_3, respectively (Figure 2C). The Eu_3O_4 field therefore is larger than in Fig. 1 and the EuS-Eu_2O_3 border is shifted to the experimental area.

Figure 1, 2B and 2C qualitatively exhibit the same phase relations with EuS in equilibrium with EuO, Eu_3O_4 and Eu_2O_2S as is shown in Fig. 3. The three phase fields, a—i, exhibit the $f(O_2)$ and $f(S_2)$ fugacities of the points a—i of Fig. 1 or at somewhat different values in Fig. 2B and C. If the phase relations of Fig. 2B are used the Eu_3O_4 and Eu_2O_2S phases would be missing. As depecticed in Fig. 2C the Eu_2O_2S field does not extend to the liquid sulfur

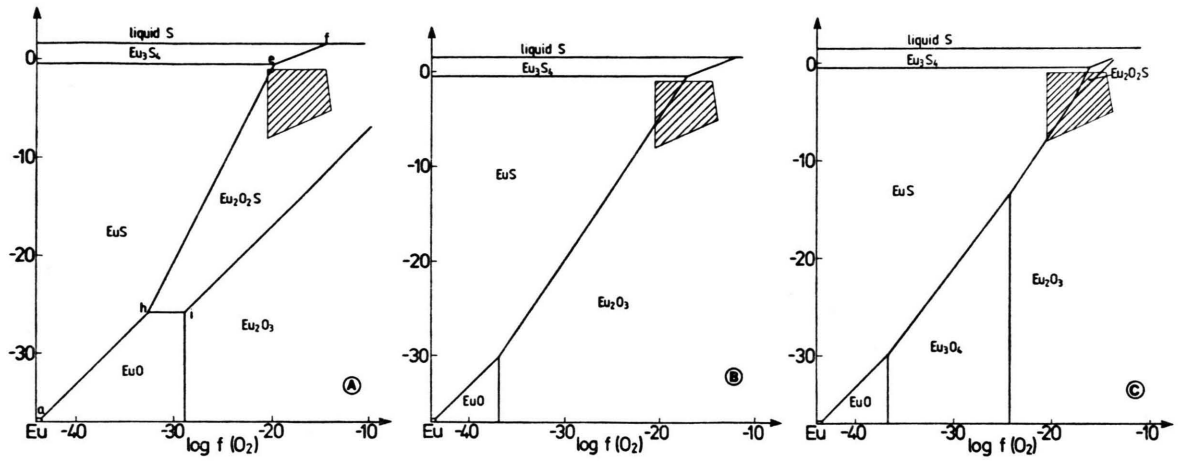

Fig. 2. Alternative phase relations of Eu-O-S phases at 900 °C as calculated from different thermodynamic data (see text).

stability field so that Eu_2O_2S would be in equilibrium with Eu_3S_4 and Eu_2O_3 which is impossible besides the phase assemblage Eu_2O_2S-EuS-Eu_2O_3 (Figure 3 I). If the coexisting phases EuO and Eu_2O_2S (Fig. 2A) are incorporated another phase diagram is produced, Figure 3 II. Solid state reactions of EuO/Eu_2O_2S mixtures in sealed quartz ampoules at 900 °C confirmed the phase relations of Fig. 3 I with EuS and Eu_2O_3 coexisting as the reaction product.

Calculations of the thermodynamic data of 1800 K with the same sources as for Fig. 1 indicates qualitatively unchanged phase relations, the reaction line VII of coexisting phases Eu_2O_3 and EuS

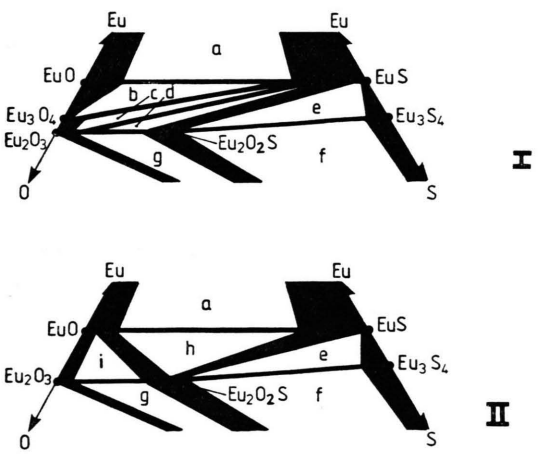

Fig. 3. Schematical phase diagrams of Eu-O-S system with the three phase fields a—i; phase diagram I for the phase relations of Fig. 1, 2B and C, II for the phase relations of Figure 2A.

however has decreased to such an extent that at higher temperatures EuS might not stay in equilibrium with Eu_2O_3, but prefer the coexistence of Eu_3O_4 and Eu_2O_2S or even EuO and Eu_2O_2S as is depecticed in Figure 3 II.

Figure 1 also includes the $f(S_2)$ partial pressure of congruently evaporating EuS as measured by Knudsen cell mass spectroscopy [23]. The composition of this compound exhibits a slight sulfur deficiency with a formula $EuS_{0.999}$, if compared to EuS at 2000 K, which was taken as stoichiometric standard. The Gibbs free energy of EuS as derived from these data $G^{298}(EuS) = -488.75$ kJ/gfw is slightly more negative than the data of [16] with $G^{298}(EuS) = -476.21$ kJ/gfw. The high temperature data of McMasters et al. [24] can be evaluated to a slightly less negative $G^{1173}(EuS) = -585.89$ kJ/gfw than $G^{1173}(EuS) = 600.25$ kJ/gfw of [16]. The slightly different values for EuS would change the phase relations only by small differences which is not relevant for the qualitative type of phase diagram.

In this investigation the phase boundary between EuS and Eu_2O_2S is considered to be accurate, because of the very sensitive method of changing $f(O_2)$ and $f(S_2)$ fugacities in small intervalls by gas-mixing. Also the Eu border line is considered to be accurate because of the feasibility to calculate thermodynamic data of the elements. The connecting reaction lines V, VI and VII between these values might have small changes in length but will retain their similar slopes.

Composition of EuS Samples

From Fig. 1 one can see that EuS exists within a wide range of $f(S_2)$ and $f(O_2)$ values and thus can exist in different stoichiometries. Holtzberg et al. [10] had shown by neutron activation analysis that single phase EuS prepared by reaction of Eu_2O_3 with H_2S at 900—1900 °C contains up to 400 ppm oxygen at 900 or 1900 °C and a minimum of 6 ppm oxygen at 1300 °C. It can be shown from thermodynamic data that the equilibrium phase by this method of preparation is near the phase boundary between Eu_3S_4 and Eu_2O_2S at 900 °C. At increased temperatures the composition moves further into the EuS field. Ishikawa et al. [4] reported 0.2—0.3 mol% O content for EuS samples prepared from Eu_2O_3 by reaction with CS_2 at 900—1000 °C at sulfur pressures which are close to the boundary to Eu_3S_4. McMasters et al. [24] analysed 1.27 mol · % O for EuS single phase samples prepared from the elements which were obviously contaminated by oxygen impurities. EuS prepared from the elements and especially samples with a slight Eu excess can increase the oxygen content by O impurities to point a of Fig. 1, where the maximum solubility of EuO in EuS is reached. The S-content of EuS should vary between the approximate composition $EuS_{0.99}$ for samples near the Eu field to $Eu_{0.97}S$ for samples near the Eu_3S_4 field [23]. The Eu^{3+} content in EuS samples prepared from $EuSO_4$ and H_2S, that is at high $f(S_2)$ and $f(O_2)$, should be less than 2% [25].

The lattice parameter of the different samples of this investigation varied by $\Delta a/\Delta \log f(O_2) \approx 0.001$ Å and $\Delta a/\Delta \log f(S_2) < 0.0005$ Å, which was just detectable by the powder diffraction method. The x-ray data are in accordance with the sketch shown in Fig. 1, with a maximum lattice constant at the stoichiometric composition EuS and different directions of decreasing lattice constants:

(1) At oxidation of some Eu^{2+} to Eu^{3+} and subsequent formation of Eu^{2+} interstices to balance the charges. The resulting formula would be $Eu_{1-x}S$ (e.g. $Eu_{0.97}S$ for samples near the Eu_3S_4 field [23].

(2) EuS forms a limited solid solution with EuO. The 1100 °C limits were determined by the solid state reaction of the Eu/Eu_2O_2S mixture to the EuS-EuO solid solution. The phase boundaries are at less than 2 mol % on both sides, if a linear interpolation of the lattice constants is assumed. The oxygen content of the solid solution $EuS_{1-y}O_y$ should increase towards the EuO field of Figure 1.

(3) At very small $f(O_2)$ and $f(S_2)$, EuS might exhibit S^{2-} vacancies and subsequently Eu at Eu^{2+} interstices, if compared to other rare earth chalcogenides [2]. This can be expressed by the formula EuS_{1-z}, e.g. $EuS_{0.99}$ for samples near the Eu field [23].

[1] T. B. Reed and R. E. Fahey, J. Crystal Growth **8**, 337 (1971).
[2] E. Kaldis, J. Crystal Growth **9**, 281 (1971).
[3] S. van Houten, Physics Letters Amsterdam **2**, 215 (1962).
[4] H. Ishikawa, M. Nakane, and Y. M. Yake, Nippon Kagaku Kaishi **1**, 56 (1973).
[5] H. Pink, Z. anorg. allg. Chem. **364**, 248 (1969).
[6] G. Sallavuard and R. A. Pâris, C. R. Acad. Sci. Paris **271**, 1460 (1970).
[7] G. Beck and W. Nowacki, Naturwiss. **26**, 495 (1938).
[8] L. Kh. Kravchenko, V. V. Sokolov, T. E. Solova, and Yu. A. Stonoga, Inorg. Mater. **9**, 117 (1973).
[9] W. Klemm and H. Senff, Z. anorg. allg. Chem. **241**, 259 (1939).
[10] F. Holtzberg, T. R. McGuire, T. Penney, M. W. Shafer, and S. von Molnar, Technical Report, IBM Watson Research Center Yorktown Heights (1971).
[11] L. Domage, J. Flahaut, and M. Guittard, C. R. Acad. Sci. Paris **249**, 697 (1959).
[12] J. Hauck and B. Cheynet, unpublished calculations of Thermodata, St. Martin-d'Hères, France.
[13] R. H. Nafziger, G. C. Ulmer, and E. Woermann in "Research Techniques for High Pressure and High Temperatures" (G. C. Ulmer, ed.) Springer-Verlag, Berlin 1971, p. 9.
[14] K.-H. Klatt, S. Pietz, and H. Wenzl, Z. Metallkunde **69**, 170 (1978).
[15] C. E. Wicke and F. E. Block, Thermodynamic Properties of 65 Elements — their Oxides, Halides, Carbides and Nitrides, Bureau of Mines Bulletin 605, Washington 1963.
[16] I. Barin and O. Knacke, Thermochemical Properties of Inorganic Substances, Springer-Verlag, Berlin 1973.
[17] K. A. Gschneidner, Jr., N. Kippenhan, and O. D. McMasters, Thermochemistry of the Rare Earths, Report IS-RIC-6, Iowa State University, Ames, Iowa 1973.
[18] N. I. Lobachevskaya, V. G. Bamburov, L. D. Finkel'shtein, N. N. Efremova, and N. D. Yakovleva, Izv. Akad. Nauk. SSR, Neorg. Mater **12**, 1187 (1976).
[19] D. H. Speidel, E. F. Heald, Bull. of the Earth and Mineral Sciences, Pennsylvania State University **83** (1967).
[20] M. W. Shafer, J. B. Torrance, and T. Penney, J. Phys. Chem. Solids **33**, 2251 (1972).
[21] R. G. Bedford and E. Catalano, J. Solid State Chemistry **3**, 112 (1971).
[22] G. J. McCarthy and W. B. White, J. Less-Common Metals **22**, 409 (1970).
[23] S. Smoes, J. Drowart, and J.-M. Welter, J. Chem. Thermodynamics **9**, 275 (1977).
[24] O. D. McMasters, K. A. Gschneidner, Jr., E. Kaldis, and G. Sampietro, J. Chem. Thermodynamics **6**, 845 (1974).
[25] M. Maletta and G. Crecelius, Appl. Phys. **8**, 241 (1975).